Electron paramagnetic resonance in $Cd_{1-x}Mn_xS$, $Cd_{1-x}Mn_xSe$, and $Cd_{1-x}Mn_xTe$

N. Samarth* and J. K. Furdyna*
Department of Physics, Purdue University, West Lafayette, Indiana 47907
(Received 20 July 1987)

We present results of a systematic investigation of EPR in the Cd-based family of diluted magnetic semiconductors ($Cd_{1-x}Mn_xS$, $Cd_{1-x}Mn_xSe$, and $Cd_{1-x}Mn_xTe$) over a wide range of temperature and Mn concentration. The dependence of the EPR linewidth on the anion of the host lattice is established. Specifically, we find that, at a fixed temperature and Mn concentration, the linewidth increases in the order of sulfide, selenide, and telluride. This trend holds over a wide range of sample composition and temperature. We also demonstrate that the general EPR behavior in all three alloys is identical: namely, the absorption line shape is Lorentzian in the paramagnetic region of the phase diagram, and broadens with increasing x and decreasing T. The Lorentzian-regime line shape is analyzed using the exchange-narrowing picture. The observed dependence of the EPR linewidth on the anion cannot be explained by dipolar broadening alone. We argue that the dominant anisotropic spin-spin interaction must be the anisotropic part of the exchange interaction, and speculate that the Dzyaloshinski-Moriya interaction may play a role. The exchange-narrowing theory is also used to examine the variation of the linewidth with sample composition and temperature. At very low temperatures, as the spin-glass transition is approached, the line shape deviates from Lorentzian behavior and the resonance appears to shift to lower fields. These non-Lorentzian line shapes are discussed with reference to similar behavior in other spin-glasses.

I. INTRODUCTION

The term "diluted magnetic semiconductors" (DMS's) commonly refers to alloys which are formed by randomly distributing magnetic ions (usually, Mn^{2+}) on the cation sites of a II-VI semiconductor such as CdTe.[1] In this paper, we focus on the Cd-based subset of this system, which consists of the wide-gap alloys $Cd_{1-x}Mn_xTe$, $Cd_{1-x}Mn_xSe$, and $Cd_{1-x}Mn_xS$. One of the fundamental problems in the study of DMS's is to understand the mechanism underlying the Mn^{2+}-Mn^{2+} interaction, and the specific aim of the present paper is to investigate this problem by studying the dynamics of the Mn^{2+} spin system via electron paramagnetic resonance (EPR).

EPR in wide-gap DMS's is a phenomenon characterized by very pronounced and yet remarkably simple dependence on temperature and sample composition. In principle, an investigation of the spin dynamics gives access to information about the nature of the spin-spin interactions, about the distribution of internal fields, and about spin-spin correlations. These properties are especially important in order to understand the different magnetic phases[1] (paramagnetic, spin-glass, antiferromagnetic cluster) that the materials display. Apart from providing insights into the fundamental physics involved, the dynamical magnetic properties are also vital in determining the switching time of potential DMS-based devices which depend on the ability of the magnetization to respond to a driving field.[2]

Earlier investigations of EPR in $Cd_{1-x}Mn_xTe$ and $Cd_{1-x}Mn_xSe$ have established the following systematic behavior:

(i) the EPR line broadens dramatically as the temperature is lowered and as the Mn concentration is increased.[3-6]

(ii) The EPR line shape is Lorentzian except in samples with a high Mn concentration at low temperatures, where there is a deviation from Lorentzian behavior accompanied by a shift of the resonance position to lower fields.[3-6]

(iii) At a fixed temperature, for samples with a Mn concentration of around 10%, the EPR linewidth shows a clear dependence on the anion in the system: namely, given a fixed cation (e.g., Cd^{2+}), the linewidth *increases* with *increasing* anion size (i.e., in the order, $Cd_{1-x}Mn_xS$, $Cd_{1-x}Mn_{1-x}Se$, $Cd_{1-x}Mn_xTe$).[7]

Despite the reproducibility and apparent simplicity of the phenomena described above, there has been little progress in developing a *theoretical* understanding of the problem. Given the germinal stage of the problem, the most profitable path to take is to exploit the striking universality of the behavior of EPR in different DMS's in the hope of identifying common trends. Bearing this aim in mind, we present a comparative study of EPR in the three systems $Cd_{1-x}Mn_xTe$, $Cd_{1-x}Mn_xSe$, and $Cd_{1-x}Mn_xS$, in which the cation is common and the anion is the "variable."

So far, the only theoretical picture of EPR line shape in DMS's is a phenomenological model proposed by Sayad and Bhagat,[5] where the Lorentzian nature of the EPR line shape is attributed to inhomogeneous broadening by a Lorentzian distribution of random local magnetic fields. Though this model is consistent with the observed phenomena and provides a useful way of empirically systematizing the data, it does not explicitly involve any microscopic parameters, such as the exchange con-

stants characterizing interactions between Mn^{2+} spins. We believe that the EPR data are more profitably examined within the context of the well-known exchange-narrowing model of EPR, as developed by Anderson and Weiss,[8] Kubo and Tomita,[9] and Mori and Kawasaki.[10]

There are two compelling reasons to view the EPR as being exchange narrowed: first, the line shape is *Lorentzian* and, second, the isotropic exchange between a pair of Mn^{2+} ions is very large (J is around 10 K). We will use the theory of exchange narrowing to examine the dependence of the EPR linewidth on the anion, on the Mn concentration, and on temperature. The anion dependence allows us to address an important issue: can the EPR linewidths in DMS's be attributed to the exchange narrowing of a dipolar-broadened resonance [as in MnO and MnS (Ref. 11), and in $Eu_xSr_{1-x}S$ (Ref. 12)], or is there some other form of anisotropic pair interaction that dominates over the magnetic dipole-dipole interaction? This issue has never been addressed in DMS's, and we shall show that the EPR data cannot be explained by dipolar broadening. Finally, we shall briefly discuss how the exchange-narrowing model can serve as a starting point for understanding the low-temperature EPR line shape.

II. EXPERIMENTAL PROCEDURE

Since the EPR line in DMS's becomes extremely broad at low temperatures, standard cavity techniques can provide reliable data only over a limited temperature range. For instance, the full width at half maximum (FWHM) of the resonance in $Cd_{0.6}Mn_{0.4}Te$ is already about 6 kG at 100 K, and continues to broaden as the temperature is further decreased. This difficulty was surmounted by using a novel 35-GHz microwave transmission spectrometer developed by Kremer and Furdyna.[3] In this method, a polarized microwave beam is passed through a sample which completely fills the cross section of a circular waveguide. In our case, the samples were in powdered form. We then measure the Faraday rotation and ellipticity of the transmitted wave as a function of an external magnetic field which is applied along the direction of propagation of the microwaves. The technique is especially suited for the measurements of very broad resonances, and can in fact be used to obtain the dynamic magnetic susceptibility under the extreme condition when the linewidth exceeds the value of the field at which the resonance occurs. Details of this method may be found elsewhere.[13] We can selectively measure either the Faraday rotation θ_f or the Faraday ellipticity ϵ_f, which are given by[3]

$$\theta_f = \frac{\omega d}{4c}(\kappa_1)^{1/2}(\chi'_+ - \chi'_-) , \tag{1a}$$

$$\epsilon_f = \frac{\omega d}{4c}(\kappa_1)^{1/2}(\chi''_+ - \chi''_-) , \tag{1b}$$

Where ω is the microwave frequency in rad/sec, d is the sample thickness (in the case of a powder, the effective sample thickness) and κ_1 is the dielectric constant of the sample. χ_+ and χ_- refer to the dynamic magnetic susceptibility for opposite circular polarizations, with the prime and double prime indicating the real and imaginary parts, respectively. The spectrometer can also be used to study narrow resonances by simply recording the transmission of a microwave beam which is polarized in the resonance-active (" + ") sense. When using circular polarization, the transmitted microwave power is given by

$$y = y_0 \exp\left[-\frac{\omega}{c}(\kappa_1)^{1/2}\chi''_+ d \right] . \tag{2}$$

All the above expressions assume single passage of the microwaves through the sample. Both the Faraday rotation-ellipticity approach and the circular polarization method were used because of the immense range of linewidths encountered (from around 150 G to around 20 kG). The circular polarization method was typically employed for resonances with FWHM less than 700 G. The analysis of the data is described in the next section.

The sample holder section of the spectrometer was mounted inside a Janis Supervaritemp Dewar. The temperature of the sample could be varied between 1.3 and around 250 K, and was measured using a calibrated silicon diode. For measurements above 4.2 K, stability to within a degree Kelvin was achieved using a Lake Shore Cryotronics capacitance bridge controller. Measurements below 4.2 K were made by immersing the sample directly in liquid helium and pumping on the helium bath.

The composition of the various samples was obtained by exploiting the linear dependence of the lattice parameter on Mn concentration for the various DMS's (Vegard's Law).[14] Lattice parameter measurements were obtained using x-ray powder diffraction patterns from a Siemens diffractometer, and a standard lattice parameter refinement program was used to calculate the best fit to the data. The typical accuracy of the lattice parameter measurements was about ± 0.001 Å; in $Cd_{1-x}Mn_xTe$, for instance, this corresponds to an error or around ± 0.006 in the value of the Mn concentration x. The quality of the diffraction patterns and the standard deviation in the calculated values of the lattice parameters also gave some indication about the homogeneity of the samples used.

We attempted to cover as wide a range of Mn concentration as possible in each of the three materials. The upper limit on Mn concentration for which it is possible to grow single-phase, homogeneous samples varies from system to system: the maximum possible value of x for $Cd_{1-x}Mn_xTe$ is ≈ 0.75 while for $Cd_{1-x}Mn_xSe$ it is $x \approx 0.50$. All the $Cd_{1-x}Mn_xTe$ and $Cd_{1-x}Mn_xSe$ samples were grown as single crystals by the Bridgman process. In both case, x-ray powder diffraction measurements indicated good homogeneity. The third material, $Cd_{1-x}Mn_xS$, is still fairly new and it is difficult to obtain good quality single crystals, particularly for $x > 0.15$. The samples of $Cd_{1-x}Mn_xS$ used in the present study were either prepared by sintering or as polycrystalline materials. X-ray diffraction measurements showed some inhomogeneity for both methods of preparation. For example, in the samples which yielded diffraction patterns of good enough quality for lattice parameter measure-

ments, the standard deviation in the values of x was about ± 0.01.

III. ANALYSIS OF FARADAY EFFECT DATA

In order to extract meaningful parameters from the EPR data, we need a model for the dynamic magnetic susceptibility which appears in Eqs. (1) and (2). This is provided by the well-known Bloch equations of motion, modified to take into account the short relaxation times associated with broad resonance lines:[3,15]

$$\frac{d\mathbf{M}}{dt}=\gamma\mathbf{M}\times\mathbf{H}-\frac{\mathbf{M}-\chi_0\mathbf{H}}{\tau} . \tag{3}$$

Here, γ is the gyromagnetic ratio ($ge/2mc$), τ is the relaxation time, and $\mathbf{H}$ is the *total* magnetic field $\mathbf{H}_0+\mathbf{H}_1$, where $\mathbf{H}_0$ is the dc field applied along the z direction and $\mathbf{H}_1$ is the microwave field. Note that the magnetization $\mathbf{M}$ relaxes to the *instantaneous* value $\chi_0\mathbf{H}(t)$ rather than to the steady-state value $\chi_0\mathbf{H}_0$ as in the standard Bloch equations. The above equations yield the following form of the dynamic magnetic susceptibility:

$$\chi'_{\pm}=\chi_0\frac{1+\omega_0(\omega_0\mp\omega)\tau^2}{1+(\omega_0\mp\omega)^2\tau^2} , \tag{4a}$$

$$\chi''_{\pm}=\chi_0\frac{\omega\tau}{1+(\omega_0\mp\omega)^2\tau^2} , \tag{4b}$$

where ω_0 and ω are the Larmor precession and microwave frequencies, respectively. Two points are worth noting about the form of the dynamic magnetic susceptibility obtained from the modified Bloch equations. First, the resonance described by the χ''_+ itself is *Lorentzian*, and, second, this resonance shows *absorption at zero field*. This absorption is negligible when the resonance is narrow, but increases in importance as the resonance broadens, as in the case at hand. The FWHM of this Lorentzian absorption line shape is given by $2/\gamma\tau$ and the peak is centered at a resonance field given by ω/γ. Note, however, that the line shapes observed in Faraday rotation and/or ellipticity experiments are combinations of the sort $\chi''_+-\chi''_-$ and $\chi'_+-\chi'_-$ and hence are not Lorentzian in shape themselves. Thus when we describe an experimental line shape as being Lorentzian, we only refer to the absorptive part of the dynamic susceptibility χ''_+.

Expressions for the Faraday rotation and ellipticity are obtained by combining Eqs. (1) and (4). The experimental line shapes are fitted to these expressions using as parameters the g factor, the relaxation time τ, and the static susceptibility χ_0. The first two parameters, g and τ, are the most important since they can be determined with little ambiguity. Further, these two parameters are related to the conventional EPR measurables of resonance position and linewidth. The last parameter, χ_0, is determined only to within a multiplicative constant because we do not have a precise way of calculating the effective thickness d of a powdered sample. In this paper, we concentrate on the parameters g and τ. The static susceptibility will be lumped along with the rest of the constants into a multiplicative parameter C given by $\omega d(\kappa_1\chi_0)^{1/2}/4c$.

Although the experiment should in principle yield purely the Faraday rotation or the Faraday ellipticity, a close examination of the data show that we actually observe a mixture of the two; a similar mixture of χ''_+ and χ'_+ occurs in the circular polarization data. For example, when we set up the experiment to measure the Faraday ellipticity ϵ_f, we actually obtain the admixture $\epsilon_f+f\theta_f$, where f is a mixing fraction that is typically about 0.1 but has been found to take values anywhere between 0 and ± 0.7. This admixture of dispersive and absorptive effects is due to several reasons, such as multiple passage of the microwaves through the sample, arising from reflections either at sample boundaries or at regions of the waveguide external to the sample; another possibility is that we do not see "pure" effects because of distortions in the waveguide which lead to imperfect polarization. To a first approximation, both of these systematic errors can be accounted for in the following way:

$$\theta(\text{observed})=\frac{\omega d}{4c}(\kappa_1)^{1/2}[(\chi'_+-\chi'_-)+f(\chi''_+-\chi''_-)]$$

$$=\theta_f+f\epsilon_f . \tag{5}$$

A more detailed discussion of this may be found elsewhere.[13] The best justification for using the assumption of such a mixture is the excellent quality of fits to the data, as we shall show later.

Thus, in the analysis which follows, four fitting parameters have been used: the g factor, the relaxation time τ, the mixing fraction f, and a multiplicative factor C described earlier. Of these, g is very close to 2 (except at low temperatures, as will be clarified later); C affects the amplitude, but not the line shape. The principal quantities which affect the line shape are then τ and f.

IV. RESULTS AND DISCUSSION

A. Survey of data

The EPR behavior in all the compounds is qualitatively identical; a representative set of the data is shown in Fig. 1. The solid lines are fits to the modified Bloch model, as discussed earlier, and the parameters used for these fits are given in Table I. For the sample shown, we obtain excellent fits for $T>20$ K, indicating that the resonance is Lorentzian over a wide range of temperatures. In this Lorentzian regime, the resonance occurs around 12.5 kG, corresponding to a g factor of 2.0 ± 0.01. Further, the resonance broadens dramatically as the temperature is lowered, without any noticeable resonance shift. The variation of the linewidth with x, T, and the anion is shown in Fig. 2 for the Lorentzian regime. In order to provide a better feel for the linewidths involved, we have converted the inverse relaxation times into FWHM in kG in the figure. The parameter τ—and consequently the linewidths—are determined to an accuracy of $\pm 5\%$.

The qualitative trends in the Lorentzian regime are clear. First, there is the dramatic broadening of the resonance as T decreases or as x increases. Second, there is a systematic dependence of the linewidth on the nature of

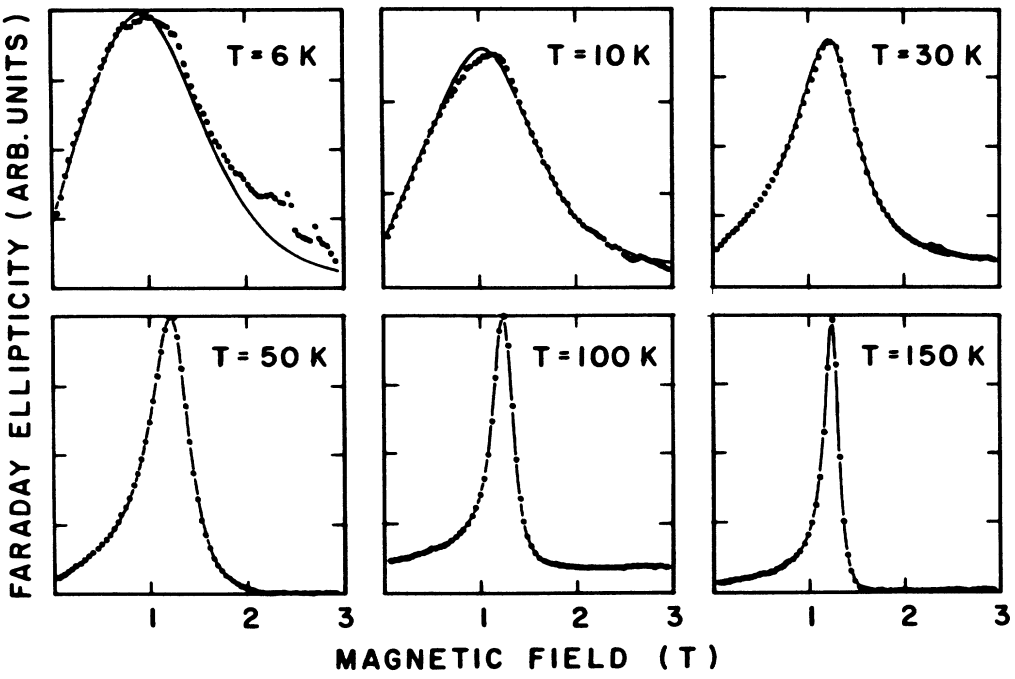

FIG. 1. Variation of EPR line shape with temperature, shown through Faraday ellipticity behavior in a $Cd_{1-x}Mn_xTe$ sample with $x=0.32$. The trends shown here are typical of all the Cd-based alloys studied. The solid lines are best fits to the modified Bloch model, and the fitting parameters are given in Table I.

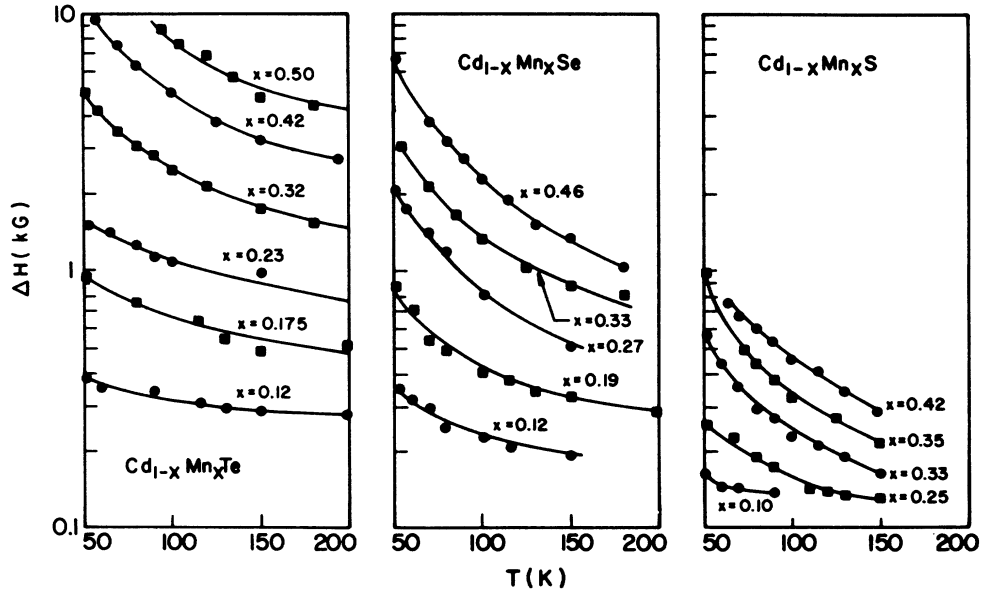

FIG. 2. The dependence of the FWHM of the Lorentzian absorption line shape on temperature and Mn concentration in the alloys $Cd_{1-x}Mn_xTe$, $Cd_{1-x}Mn_xSe$, and $Cd_{1-x}Mn_xS$. This figure also clearly shows the dependence of the linewidth on the anion. Data for other values of x agree with the curves shown (e.g., ΔH for $x=0.25$ would lie between $x=0.3$ and $x=0.2$ data), but is omitted for clarity.

TABLE I. Parameters employed in fitting line shapes shown in Fig. 1.

T (K)	C (10^{-3})	g	τ (10^{-11} sec)	f
6	4.5	2.4	0.47	−0.50
10	3.5	2.2	0.67	−0.40
30	4.1	2.0	1.43	−0.28
50	3.8	2.0	4.35	−0.33
100	3.2	2.0	4.70	−0.25
150	2.4	2.0	6.50	−0.30

the anion, i.e., for a given x and T, the linewidth increases in the order $Cd_{1-x}Mn_xS$, $Cd_{1-x}Mn_xSe$, $Cd_{1-x}Mn_xTe$. Note that the trend in the anion dependence holds over a wide range of x and T, confirming the predictions of Kremer and Furdyna.[7]

At very low temperatures, we find that the fits to the modified Bloch model gradually get worse, as can be surmised from Fig. 1, indicating a departure from Lorentzian behavior. Since the Faraday effect data consist of combinations of χ'_+, χ'_-, χ''_+, and χ''_-, it is not possible to draw ready conclusions about the low-temperature line shape—such as whether the absorption χ''_+ is symmetric or not. We have found, however, that the data cannot be fitted to a simple model for χ''_+, such as a Lorentzian or Gaussian. If we force a fit to a Lorentzian model, as in the lowest-temperature data in Fig. 1, the maximum of the Lorentzian has to be positioned at fields lower than 12.5 Kg, indicating a resonance shift at low temperatures. The resonance shift can be modeled either by adjusting the g factor or by using an internal field as an extra parameter. Since neither method provides very good fits, we have arbitrarily chosen the former option in Table I.

All of the above results confirm earlier work in $Cd_{1-x}Mn_xTe$ (Refs. 3–5) and $Cd_{1-x}Mn_xSe$ (Ref. 6), and also show that essentially the same behavior is found in $Cd_{1-x}Mn_xS$. In the discussion that follows, we systematize the dependence of ΔH on the anion, on T, and on x, and examine these trends from the vantage point of exchange narrowing. Finally, we examine the implications of the non-Lorentzian line shapes at low temperatures.

B. The Lorentzian regime

In general, the exchange-narrowed EPR line shape is Lorentzian, and, at a temperature T, the FWHM (ΔH) can be written as (see the Appendix for comments)[16]

$$\Delta H = (\Delta H)_\infty (T\chi_0)^{-1}\Gamma(T,x) , \tag{6}$$

where χ_0 is the static susceptibility. The infinite temperature linewidth $(\Delta H)_\infty$ is given by[8]

$$(\Delta H)_\infty = \frac{2}{\gamma}\frac{\omega_d^2}{\omega_e} , \tag{7}$$

where ω_d and ω_e are measures of the anisotropic and isotropic spin-spin interactions, respectively, and can be obtained from moment method calculations.[17] The function $\Gamma(T,x)$ depends on dynamic spin-spin correlations. While we do not have an analytic form for $\Gamma(T,x)$, it is reasonable to assume that the function will be temperature independent when $T \gg T_g$, where T_g is the spin-glass transition temperature in a DMS. When this is so, the Curie-Weiss behavior of the high-temperature susceptibility[18] in the DMS should result in a linewidth which has the following temperature dependence:

$$\Delta H = (\Delta H)_\infty \left(1+\frac{\Theta}{T}\right) , \tag{8}$$

where Θ is the Curie-Weiss temperature. Thus a comparison between theory and experiment can be made by extrapolating a plot of ΔH versus $1/T$ to obtain the experimental value of $(\Delta H)_\infty$.

An alternative way to compare theory and experiment is to assume that (ΔH) is a universal function of the reduced temperature $T' = kT/J$, i.e.,

$$\Delta H = (\Delta H)_\infty g[T',x] . \tag{9}$$

At high temperatures, the above ansatz is equivalent to the temperature dependence in Eqs. (6) and (8), since $\Gamma(T,x)$ is temperature dependent and Θ is proportional to J in a mean-field approach. The ratio of linewidths in two different systems with the same Mn concentration x at the same reduced temperature T' can then be directly compared to the theoretical ratio at infinite temperature.

1. *The anion dependence of the linewidth*

In order to focus on the anion as the variable, the discussion here is restricted to three of the samples shown in Fig. 2 which have approximately the same Mn concentration (around $x=0.33$). Table II lists the relevant parameters required for the analysis. The nearest-neighbor exchange constants are obtained from high-field magnetization measurements.[19,20]

We begin by assuming that the anisotropic pair interaction is the magnetic dipole-dipole interaction. Using the moment method[17] and the Anderson-Weiss approach,[8] we have calculated the exchange-narrowed, dipolar-broadened linewidth at infinite temperature for a diluted magnetic fcc lattice, assuming nearest-neighbor interactions only and an isotropic sample. The nearest-neighbor approximation renders the calculation applicable to a hcp lattice as well. [The systems we are studying are either zinc blende ($Cd_{1-x}Mn_xTe$) or wurtzite ($Cd_{1-x}Mn_xSe$ and $Cd_{1-x}Mn_xS$), in which the Mn^{2+} ions occupy fcc and hcp sublattices, respectively.] We also include the so-called "$\frac{10}{3}$" effect due to nonsecular contributions, because of the strong isotropic exchange.[8] The FWHM at infinite temperature is then given by[13]

$$(\Delta H)_\infty \simeq \frac{22}{\gamma}\left[\frac{\gamma^4\hbar^2}{r^6}\right]\frac{\hbar}{J}\frac{x}{\sqrt{x+0.07}} , \tag{10}$$

where r is the nearest Mn^{2+}-Mn^{2+} neighbor distance in a fully occupied lattice, J is the nearest-neighbor Mn^{2+}-Mn^{2+} exchange constant, x is the concentration of Mn^{2+} ions, and γ is the gyromagnetic ratio.

We now use the ansatz given in Eq. (9). Figure 3 shows the linewidth in the three samples of interest as a func-

TABLE II. Comparison of experimental and theoretical linewidths in $Cd_{0.68}Mn_{0.32}Te$, $Cd_{0.67}Mn_{0.33}Se$, and $Cd_{0.67}Mn_{0.33}S$ at the same reduced temperature $T'=kT/J$; f_{expt}, f_{dip}, and f_{DM} are the experimental, dipolar and D-M linewidths, respectively, normalized to the corresponding linewidth in the telluride.

Sample	r_{NN} (Å)	J (K)	λ (eV)	f_{expt}	f_{dip}	$f_{D\text{-}M}$
$Cd_{0.68}Mn_{0.32}Te$	4.555	6.3	0.37	1.00	1.00	1.00
$Cd_{0.67}Mn_{0.33}Se$	4.255	7.9	0.16	0.43	1.20	0.24
$Cd_{0.67}Mn_{0.33}S$	4.088	10.6	0.025	0.06	1.14	0.008

tion of the reduced temperature $T'=T/J$. The validity of Eq. (9) at high temperatures is clear—to a good approximation, ΔH is a universal function of T' for $T'>10$. In Fig. 3, f_{expt} is the ratio $(\Delta H)_1/(\Delta H)_2$ of experimentally measured linewidths in two samples at the same value of T', where we arbitrarily choose the telluride linewidth for normalizing the others, i.e., subscript "2" corresponds to $Cd_{0.68}Mn_{0.32}Te$. The parameter f_{expt} has values of 1, 0.43, and 0.06 for the telluride, selenide, and sulfide, respectively. Theory predicts that, assuming dipolar broadening, the ratio of linewidths in two different materials at the same values of x and T' should be given by [see Eq. (10)]

$$f_{dip}=\frac{(\Delta H)_1}{(\Delta H)_2}=\left[\frac{r_2}{r_1}\right]^6\left[\frac{J_2}{J_1}\right]. \tag{11}$$

The results of the analysis using Eq. (11) are shown in Table II, where we once again have normalized to the telluride linewidth; f_{expt} is the corresponding experimentally observed ratio used in Fig. 3. Table II clearly demonstrates that dipolar broadening cannot even explain the *qualitative* variation of the linewidth as the anion is changed. Thus the dominant anisotropy which governs the behavior of the EPR linewidth cannot be dipolar in origin. The only other possible source of line broadening is the anisotropic part of the exchange interaction, for which we will propose a plausible—though speculative—form.

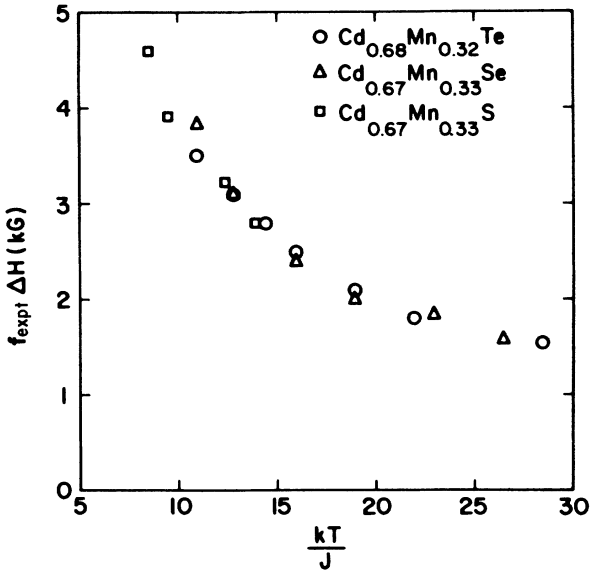

FIG. 3. The temperature variation of the linewidth in $Cd_{0.68}Mn_{0.32}Te$, $Cd_{0.67}Mn_{0.33}Se$, and $Cd_{0.67}Mn_{0.33}S$, showing that the temperature dependence follows a scale T/J. Here f_{expt} is a normalizing factor, which takes values of 1, 0.43, and 0.06 for the telluride, selenide, and sulfide, respectively.

Theoretical work by Larson *et al.*[21] indicates that the main contribution to the Mn^{2+}-Mn^{2+} exchange interaction is from superexchange. It is known that, when there is lack of inversion symmetry, a perturbation due to spin-orbit coupling within a superexchange mechanism can lead to an anisotropic exchange term known as the Dzyaloshinski-Moriya (D-M) interaction.[22] The D-M interaction is of the form $\mathbf{D}_{ij}\cdot(\mathbf{S}_i\times\mathbf{S}_j)$ and has a strength given by $D\sim\lambda J/U$, where λ is the relevant spin-orbit coupling constant of the problem, and U is an effective energy scale[21] that enters into the superexchange mechanism. The restricted symmetry condition is clearly satisfied by the zinc-blende and wurtzite structures of the DMS's. Having excluded the dipole interaction as the dominant anisotropy, the D-M interaction offers a promising alternative to explain the EPR data.[23] (This form of anisotropic exchange was also suggested by Keffer[24] in the case of β-MnS, which, like the DMS's, occurs in wurtzite and zinc-blende forms).

By repeating the moment method calculation using the D-M interaction instead of the dipole interaction, we obtain the FWHM at infinite temperature in the form[13]

$$(\Delta H)_\infty\simeq\frac{10.5}{\gamma}\left[\frac{\lambda}{U}\right]^2\frac{J}{\hbar}\frac{x}{\sqrt{x+0.1}}. \tag{12}$$

The whole D-M Hamiltonian (secular and nonsecular parts) was employed in arriving at the above result, and we have used the same approximations as earlier. Theoretically, the ratio of linewidths should now be given by

$$f_{D\text{-}M}=\frac{(\Delta H)_1}{(\Delta H)_2}=\left[\frac{\lambda_1}{\lambda_2}\right]^2\frac{J_1}{J_2}. \tag{13}$$

The value of U is expected to be similar for all Mn-based DMS's, and hence, to a first approximation, the variation of U with the anion is ignored. In the absence of a theoretical formulation for the D-M interaction in DMS's, we have to guess at the required spin-orbit coupling. The strong anion dependence of the linewidth, in conjunction with the major role played by the anions in mediating the superexchange interaction, suggests that we use the spin-orbit coupling due to the anion. (The

spin-orbit coupling from the Mn^{2+} ions should be negligible because they are in an S state.) We can then obtain the relevant spin-orbit coupling from the renormalized spin-orbit splittings Δ for the anion in a crystal environment.[25] In Table II, we have assumed that $\lambda=\Delta/3$ (Ref. 25). While the absolute values may be a little uncertain, we believe that the above numbers are a good reflection of the relative variation of λ. The drastic change in λ from one anion to another implies that the variation of ΔH with the anion is mainly determined by the spin-orbit coupling, and not by the exchange constant.

The results of the comparison are shown in Table II via the ratio f_{DM}. As before, we have normalized by the linewidth of the telluride. Although the quantitative agreement is not very good, clearly the gross trends are correctly predicted by Eq. (13). This is encouraging, given the speculation about the values of U and λ. The large discrepancy in the case of $Cd_{1-x}Mn_xS$ might arise because of the very small spin-orbit coupling for the sulfur ion. It is conceivable that, because of the smallness of λ, the dipolar forces are in this case either comparable to—or even larger than—the D-M interaction, leading to a broader line than might result solely from D-M broadening. This view can be strengthed by making an infinite temperature extrapolation.

A plot of ΔH versus $1/T$ at high temperatures yields approximate infinite temperature limits of 40, 350, and 500 G for $Cd_{0.67}Mn_{0.33}S$, $Cd_{0.67}Mn_{0.33}Se$, and $Cd_{0.68}Mn_{0.32}Te$, respectively (see Figs. 4–6). The results should be used with caution because the lack of data at sufficiently high temperatures leads to some uncertainty in the extrapolation. However, the infinite temperature linewidths predicted for dipolar broadening by Eq. (10) are around 10 G for all three cases, and we can safely conclude that the telluride and selenide linewidths are far too broad to be consistent with this theoretical result. Given the uncertainty in the linear approximation, the role of dipolar broadening in the case of the sulfide cannot be ruled out. The uncertainty in the absolute values of λ and U renders a similar comparison with the D-M linewidths difficult. Rough linewidths may be obtained by using the values of λ in Table II in conjunction with

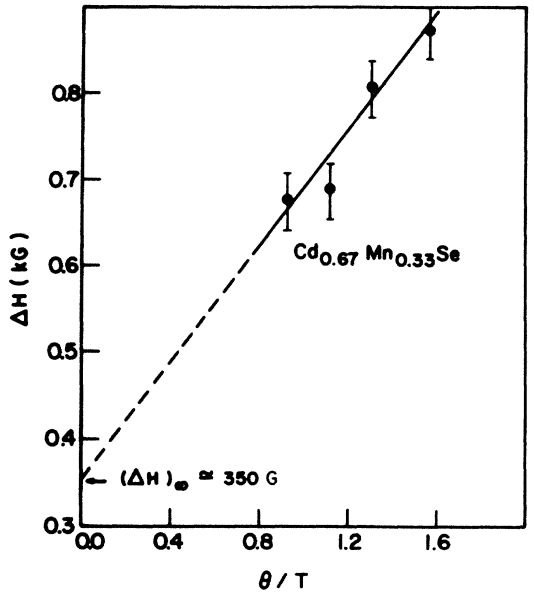

FIG. 5. Linear extrapolation of linewidth data in $Cd_{0.67}Mn_{0.33}Se$ to obtain an estimate of ΔH in the infinite temperature limit.

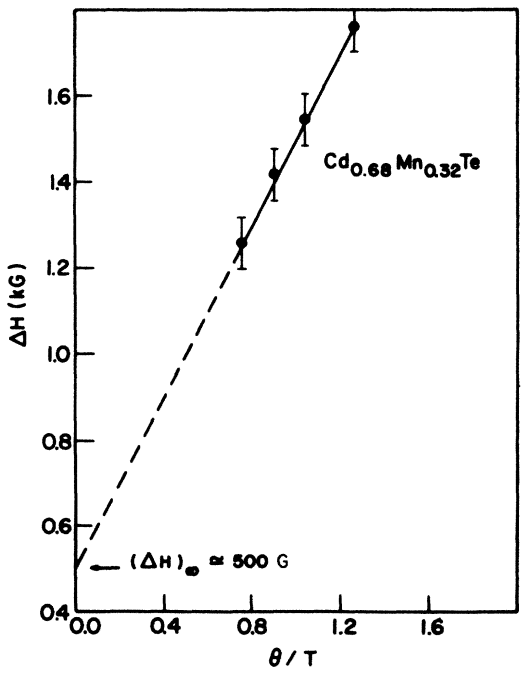

FIG. 4. Linear extrapolation of linewidth data in $Cd_{0.68}Mn_{0.32}Te$ to obtain an estimate of ΔH in the infinite temperature limit.

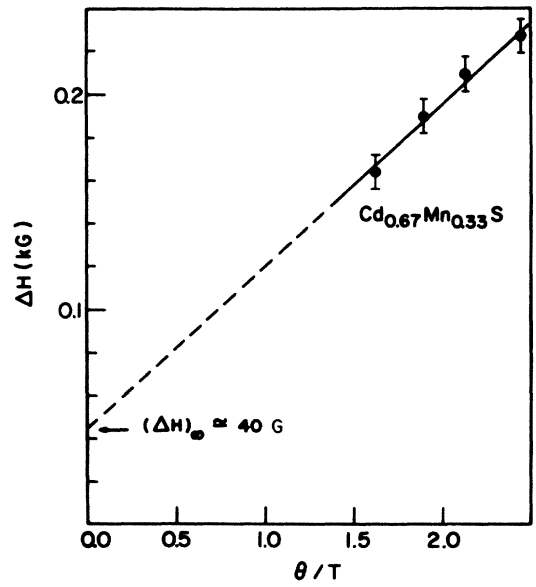

FIG. 6. Linear extrapolation of linewidth data in $Cd_{0.67}Mn_{0.33}S$ to obtain an estimate of ΔH in the infinite temperature limit.

the estimate by Larson *et al.*[21] that U is around 6 eV in $Cd_{1-x}Mn_xTe$. The infinite-temperature D-M linewidths for the telluride, selenide, and sulfide are then around 900, 200, and 7 G, respectively. The numbers are at least in the correct range required by the approximate extrapolation of the experimental data, and reinforce the case for the D-M interaction. The calculation also produces comparable D-M and dipolar contributions in the sulfide, and a detailed moment calculation which includes both interactions may yield better results.

In summary, we rule out the role of dipolar broadening by two arguments: first, by comparing the ratios between linewidths in the different materials at a finite temperature to the theoretically predicted ratios at $T=\infty$, and, second, by comparing the theoretically calculated magnitudes of $(\Delta H)_\infty$ with an estimate obtained by extrapolating finite temperature data to the infinite temperature limit. Further, the relative variation of the linewidth with the anion is consistent with the Dzyaloshinski-Moriya interaction, and the extrapolated estimates of $(\Delta H)_\infty$ are in the correct range required by the theoretical estimates using the D-M interaction.

2. *Variation of linewidth with Mn^{2+} concentration*

We now consider the dependence of the linewidth on Mn concentration x. Figures 7–9 show the linewidth as a function of x in all the Cd-based DMS's at the highest temperatures in this study. While a detailed fit to the x dependence is unwarranted at this stage, it is clear that the concentration dependence is not linear, and may be viewed approximately as obeying an x^2 law.

The x dependence predicted by Eq. (8), on the other hand, is approximately $x^{1.5}$, since there is a $\sqrt{x}$ term contribution from $(\Delta H)_\infty$ and a term linear in x from Θ—in DMS's, the Curie-Weiss temperature is approximately linear in x, i.e., $\Theta=\Theta_0 x$ (Ref. 18). More experimental work is required to proceed further. In particular, better estimates of $(\Delta H)_\infty$ need to be obtained from EPR data taken at higher temperatures (say, 250–400 K)

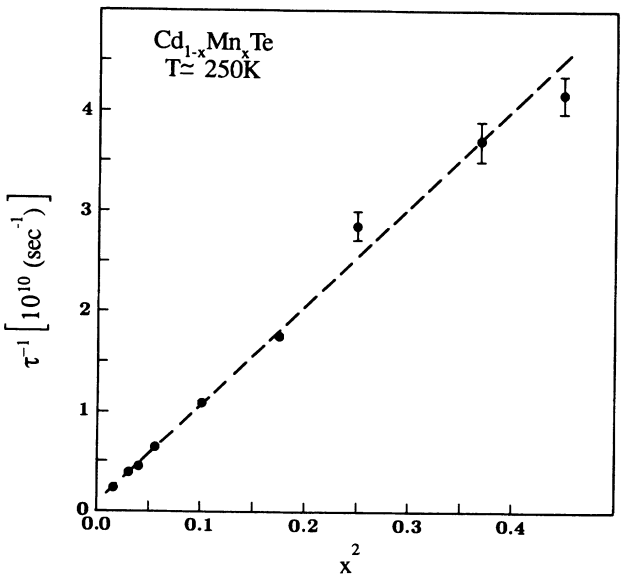

FIG. 7. Inverse relaxation time τ^{-1} (proportional to ΔH) at $T=250$ K in $Cd_{1-x}Mn_xTe$ as a function of x^2.

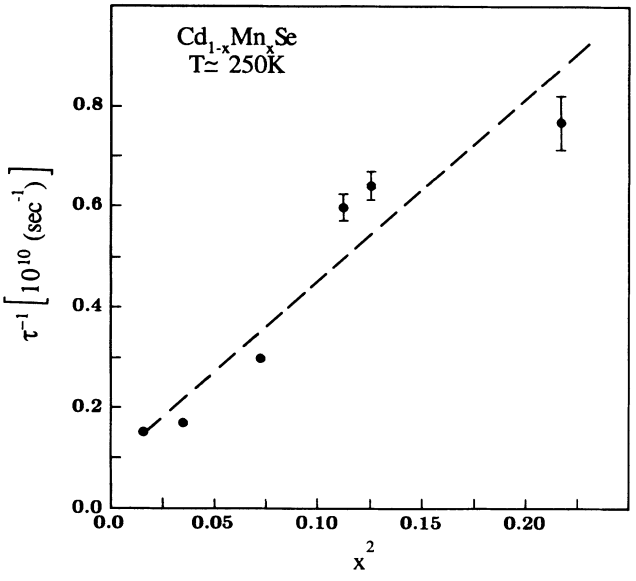

FIG. 8. Inverse relaxation time τ^{-1} (proportional to ΔH) at $T=250$ K in $Cd_{1-x}Mn_xSe$ as a function of x^2.

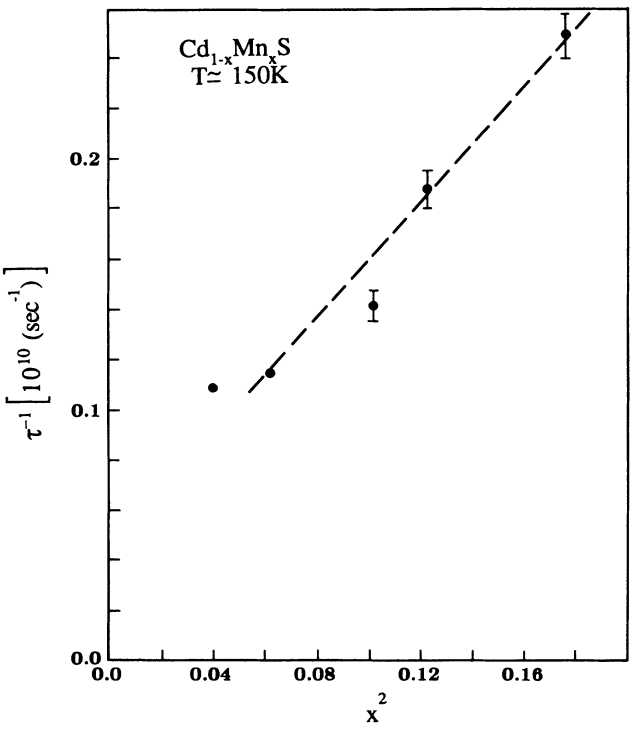

FIG. 9. Inverse relaxation time τ^{-1} (proportional to ΔH) at $T=150$ K in $Cd_{1-x}Mn_xS$ as a function of x^2.

and then examined for the concentration dependence predicted by exchange narrowing theory at $T=\infty$.

3. *The temperature dependence of the linewidth*

a. Empirical temperature dependence of ΔH. A first step towards understanding the temperature variation of ΔH would be to establish any universal behavior characterizing the phenomenon, regardless of the material and the Mn concentration. Although we have found no way of doing this for the dilute samples, our data indicate that, for samples with a high Mn concentration ($x \geq 0.20$—above the percolation threshold for nearest-neighbor interactions), the temperature dependence is empirically given by a universal function of scaled temperature:

$$\Delta H = (\Delta H)_\infty g\left[\frac{T}{T_0}\right], \tag{14}$$

where T_0 is a phenomenological scaling temperature dependent on x, and $(\Delta H)_\infty$ is characteristic of the anion of the host lattice. [Clearly, this representation is equivalent to the ansatz in Eq. (9), except that the x dependence is now absorbed into T_0.] The validity of Eq. (14) is shown in Fig. 10, where we have plotted the inverse relaxation time τ^{-1}—proportional to ΔH—as a function of T/T_0. The linewidths have been scaled by a multiplicative parameter A to collapse all the points onto a common curve, showing that the functional form is indeed universal. The values of T_0 and A employed in the plot are given in Table III. This result suggests a common mechanism underlying the broadening of the resonance with decreasing temperature in all DMS's.

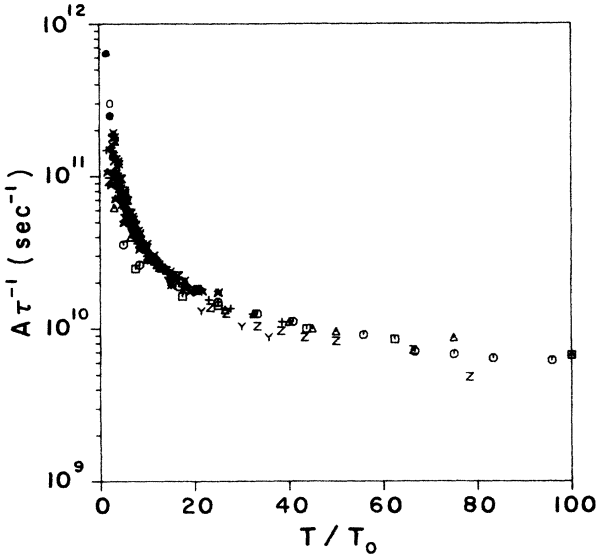

FIG. 10. This figure shows that the inverse relaxation time τ^{-1}—or equivalently the linewidth—in all the Cd-based DMS alloys, for $x > 0.20$, may be regarded as a universal function of scaled temperature. The data shown here are taken from Fig. 1, and the scaling parameters used in this plot are given in Table III. We have not provided a key to the figure since the aim is to simply illustrate that all the points can be scaled onto a common curve.

The behavior of the scaling temperature T_0 as a function of x is shown in Figs. 11–13. For comparison, the corresponding values of the spin-glass transition temperature T_g are plotted on the same graphs. Note that each set of T_0 can be multiplied by a constant and still serve as a valid scale. Each set has been chosen so as to make a comparison with the corresponding set of spin-glass temperatures. Although we cannot immediately identify T_0 with T_g since they are related by an undetermined constant, there is an intriguing correspondence between the two. This is reminiscent of the critical scaling found in other spin-glasses.[26] However, it is surprising that this scaling works for temperatures well above T_g. A similar result was obtained in the course of an early study of EPR in $Cd_{1-x}Mn_xTe$ and $Cd_{1-x}Mn_xSe$,[5] but was treated as an artifice of the empirical formula employed to fit the temperature dependence of ΔH.

b. Temperature dependence of ΔH *using the exchange-narrowing model.* Apart from such an empirical approach, we can also examine the temperature variation of ΔH using the exchange-narrowing model [Eq. (6)]. While it is difficult to obtain an analytical form for the function $\Gamma(T,x)$ from theory, we can use our experimental data to extract its qualitative behavior, by plotting $\chi_0 T(\Delta H)$ versus T. In other words,

$$\Gamma(T,x) = \frac{\Delta H(T)}{(\Delta H)_\infty}\chi_0 T\ . \tag{15}$$

Although we do not have susceptibility data for the samples used in this study, the high-temperature behavior of

TABLE III. Samples and parameters used in Fig. 10.

Alloy	A	x	$T_0(x)$ K
$Cd_{1-x}Mn_xTe$	1.0	0.175	0.8
		0.20	1.2
		0.23	2.0
		0.32	6.5
		0.42	13.0
		0.50	21.0
		0.61	27.0
		0.67	32.0
$Cd_{1-x}Mn_xSe$	2.9	0.19	3.0
		0.27	7.0
		0.33	10.0
		0.355	12.0
		0.46	15.0
$Cd_{1-x}Mn_xS$	15.0	0.25	6.0
		0.33	10.0
		0.35	14.0
		0.42	17.0

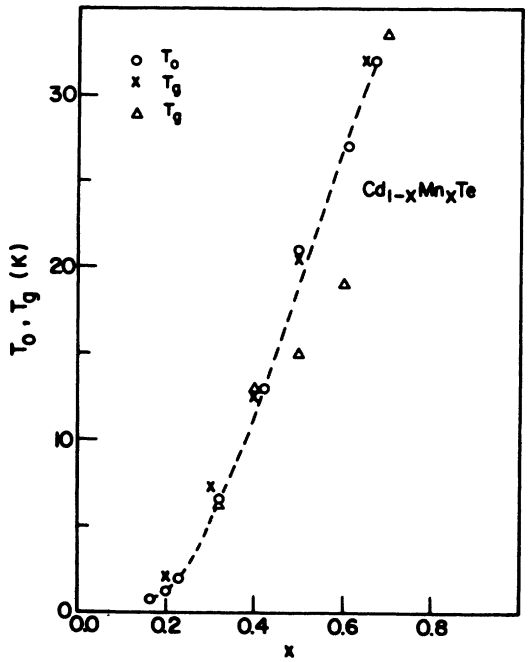

FIG. 11. Comparison between the scaling temperature T_0 and the spin-glass temperature T_g for $Cd_{1-x}Mn_xTe$. The triangles are from Ref. 31 and the crosses from Ref. 32.

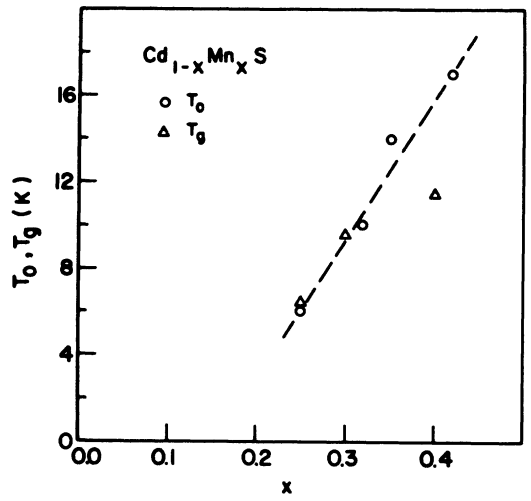

FIG. 13. Comparison between the scaling temperature T_0 and the spin-glass temperature T_g for $Cd_{1-x}Mn_xS$. The values of T_g are taken from Ref. 34.

χ_0 in the Curie-Weiss regime is systematic enough that we can borrow results from elsewhere.[18] The resulting form of $\Gamma(T,x)$ is shown for $Cd_{1-x}Mn_xTe$ in Fig. 14. The figure shows that, in the Curie-Weiss regime, the temperature variation of the dynamic spin-spin correlations is relatively slow, and that the dependence of ΔH on temperature largely reflects the temperature variation of the *static* susceptibility. For example, a comparison with Fig. 2 shows that, for the $x=0.32$ sample, the linewidth changes by over 400% over the temperature range shown, while the contribution from the dynamic spin-spin correlations changes by only 40%. However, it can be expected that as the spin-glass temperature is approached the linewidth variation will be dominated by the spin dynamics. We are not in a position to make this analysis because, at such low temperatures, the susceptibility deviates from the systematic Curie-Weiss behavior. Also, the line shape becomes non-Lorentzian, and the linewidth is no longer well defined.

C. The low-temperature line shape

The low-temperature line shape presents difficulties because of several factors. First, the resonances become so broad (FWHM >20 kG) that the associated Faraday

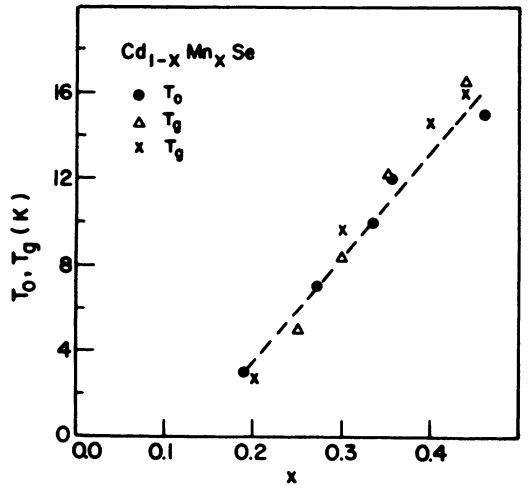

FIG. 12. Comparison between the scaling temperature T_0 and the spin-glass temperature T_g for $Cd_{1-x}Mn_xS$. The triangles are from Ref. 33 and the crosses from Ref. 32.

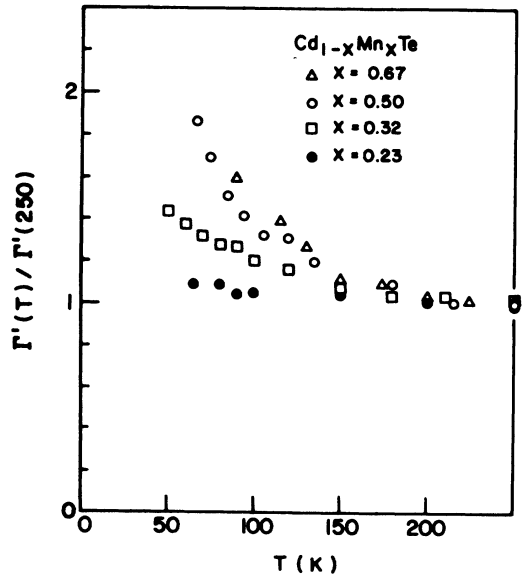

FIG. 14. Temperature dependence of the dynamic spin-spin correlations, represented by $\Gamma(T,x)$ in Eq. (6). The parameter Γ' is equal to $(\Delta H)T\chi_0$.

effect is extremely small, making it difficult to obtain reliable data. Next, in many samples it is difficult to separate any authentic changes in line shape from other spurious effects, such as the emergence of a narrow resonance superimposed on the main resonance.[3] Finally, since the Faraday line shapes are combinations of the real and imaginary parts of the dynamic susceptibility, we need a specific model to fit the line shapes in order to extract any useful information. All we can conclude from our data is that the resonance gradually deviates from Lorentzian behavior and seems to shift to lower fields.

1. *Shifted Lorentzian model*

Owing to the absence of a theoretical model for a non-Lorentzian line shape, earlier studies have treated the low-temperature EPR line shape as a shifted Lorentzian, modeled by a variable g factor[3–5] or by an internal field[6] along a preferred direction. Both approaches were used in the analysis of our data, and it was found that neither method produces significantly better results. Hence, we arbitrarily chose to fit the data shown in Fig. 1 by assuming a variable g factor. Figure 1 shows that, although the phenomenological model of a shifted Lorentzian is not bad, there is a clear deviation from Lorentzian behavior which warrants investigation.

2. *The Kubo-Toyabe model*

Superficially, the low-temperature EPR behavior described above is reminiscent of that observed in more conventional spin-glass alloys such as CuMn, AgMn (Ref. 26), and amorphous Fe-Ni-P (Ref. 27), where, as the spin-glass transition is approached, the broadening of the EPR is accompanied by a lineshift. Hou *et al.*[27] also pointed out that there is a *deviation* from the *Lorentzian* exchange-narrowed line shape, accompanied by the development of a *finite absorption* at *zero field,* which heralds important changes in the spin dynamics. This was explained using a modified version of the Kubo-Toyabe model[28] where the EPR line shape is characterized using two parameters: Δ, which is the width of a Gaussian distribution of local fields, and ν, which is the rate of exponential decay of correlations between local fields.

The Kubo-Toyabe model is the *only* existing theory which seems to predict, even *qualitatively,* the low-temperature features that we observe in DMS's, viz., both a lineshift and a non-Lorentzian line shape with zero-field absorption. However, the theory in its present form seems to be inapplicable to EPR in DMS's: the non-Lorentzian line shapes we obtain cannot be fitted very well using any combination of Δ and ν.[29]

The failure of this model indicates that some of the assumptions in the theory may be violated in our case—either the spin-spin correlations do not decay exponentially or the local-field distribution is not simply a Gaussian. However, recent μsr experiments in $Cd_{1-x}Mn_xTe$ suggest that the spin-spin correlations always show exponential relaxation—even at temperatures where the EPR line shape has ceased to be Lorentzian.[30] This leaves the possibility that the second hypothesis does not apply, and that the distribution of local fields may be deviating from a Gaussian. Another possibility is that the local-field distribution moves away from zero mean—this amounts to assuming an internal field in a preferred direction. However, we find that the introduction of an internal field as a phenomenological modification to the Kubo-Toyabe model still does not satisfactorily account for the observed line shapes.

These results indicate fundamental differences between the spin dynamics in DMS's and that in other spin-glasses. At this stage, the only reasonable conclusion we can draw is that the changes in line shape in DMS's are not simply dependent on the spin dynamics. Rather, they may signal significant changes in the distribution of local fields.

V. CONCLUSIONS

We have argued that the anion dependence of the EPR linewidth in DMS's offers vital clues about the magnetism in these materials. While there is ample systematic experimental data available, the theoretical interpretation of this data remains a challenge. The most likely resolution of the problem lies in the theory of exchange narrowing which allows the consideration of two fundamental questions: what is the dominant anisotropic pair interaction and how do the dynamic spin-spin correlations evolve with lowering temperature?

In response to the former inquiry, we have shown that the dominant anisotropy cannot be dipolar and may stem from anisotropic exchange. The exact nature of this anisotropy is still an open question, but we speculate that the solution lies in the Dzyaloshinski-Moriya interaction. A theoretical formulation of anisotropic exchange in DMS's is needed in order to substantiate the viability of this hypothesis.

The variation of the EPR linewidth and line shape with temperature bears directly on the evolution of the spin-spin correlations and the freezing of spins at low temperatures. We find that, in the paramagnetic region, the dramatic broadening of the EPR with decreasing temperature is largely due to the temperature variation of the static susceptibility. As the spin-glass region is approached, the variation of the dynamic spin-spin correlations becomes more important. Unfortunately, it is precisely in this region of interest that EPR becomes more difficult to interpret. We emphasize the importance of analyzing the EPR *line shape* in this region, because any theoretical attempts to interpret the low-temperature EPR must account for the gradual deviation of the line shape from a Lorentzian. Once again, there is need for more theoretical work in order to proceed further.

Note added in proof. We were informed, recently, of a theoretical calculation by Larson[35] confirming the importance of the D-M interaction in DMS and its role in determining EPR linewidths. Our conclusions regarding the D-M interaction are in qualitative agreement with the results of Larson's detailed calculations.

ACKNOWLEDGMENTS

We are grateful to C. Henley for providing the impetus for these ideas and would like to thank K. C. Hass, D. L. Huber, J. Kossut, B. Larson, M. B. Salamon and M. Butler for helpful suggestions and discussions. This work was supported by National Science Foundation Grant No. DMR 85-20866.

APPENDIX: COMMENTS REGARDING THE CALCULATION OF EXCHANGE-NARROWED LINEWIDTHS

Huber's formulation of the Mori-Kawasaki treatment of exchange narrowing shows that the linewidth of the Lorentzian exchange-narrowed line shape is[16]

$$\Delta H=(T\chi_0)^{-1}\mathrm{Re}\left[\sum_q A_q\int_0^\infty e^{-i\omega t}\,|\,S(q,t)\,|\,^2dt\right], \quad \text{(A1)}$$

where A_q is a coefficient which depends on the nature of the anisotropic spin-spin interactions and on the lattice structure. The factor $S(q,t)$ depends on dynamic spin-spin correlations. Since we do not have any specific information about $S(q,t)$ in DMS's, it is difficult to simplify Eq. (A1) into any useful analytic form. Consequently, we choose to formulate the linewidth as

$$\Delta H=(\Delta H)_\infty(T\chi_0)^{-1}\Gamma(T,x)\ , \quad \text{(A2)}$$

where the spin-spin correlations and the sum over q are absorbed into a function $\Gamma(T,x)$, where x is the concentration of Mn ions. All that can be reasonably assumed at this stage is that $\Gamma(T,x)$ is temperature independent at temperatures far above the spin-glass transition. While some insights into the qualitative behavior of $\Gamma(T,x)$ can be drawn from the EPR data, further progress will have to await more information on $S(q,t)$ from, say, inelastic neutron scattering measurements.

In order to calculate the infinite temperature linewidth $(\Delta H)_\infty$, we use the well-known result of Anderson and Weiss[8] and Van Vleck:[17]

$$\Delta H=\frac{(2\pi)^{1/2}}{\gamma}\frac{(M_2)^{3/2}}{(M_4')^{1/2}}\ , \quad \text{(A3)}$$

where M_2 and M_4' are given by

$$M_2=-\frac{\mathrm{Tr}([H_A,S_x]^2)}{\hbar^2\mathrm{Tr}(S_x^2)}\ , \quad \text{(A4)}$$

$$M_4'=\frac{\mathrm{Tr}([H_e,[H_A,S_x]]^2)}{\hbar^4\mathrm{Tr}(S_x^2)}\ . \quad \text{(A5)}$$

In the above expression, S_x is the x component of the total spin, H_e is the isotropic Heisenberg exchange Hamiltonian, specifically

$$H_e=-2\sum_{\substack{i,j\\ i<j}}J_{ij}\mathbf{S}_i\cdot\mathbf{S}_j\ , \quad \text{(A6)}$$

and H_A is the relevant anisotropic exchange term.

If we consider dipolar broadening, H_A has the usual form:

$$H_A=H_d=\gamma^2\hbar^2\sum_{\substack{i,j\\ i<j}}[\mathbf{S}_i\cdot\mathbf{S}_j-3(\mathbf{S}_i\cdot\hat{\mathbf{r}}_{ij})(\mathbf{S}_j\cdot\hat{\mathbf{r}}_{ij})](r_{ij})^{-3}\ . \quad \text{(A7)}$$

The linewidth ΔH is then calculated using Eqs. (A3)–(A5). We begin with the expressions for M_2 and M_4' derived by Van Vleck,[17] and then perform the calculations by assuming a randomly diluted magnetic fcc lattice. The algebra is considerably simplified by restricting exchange interactions to nearest neighbors and by averaging angular factors over the unit sphere. The latter simplification is certainly valid for a powdered sample as in the present case. The random dilution of the fcc lattice is accounted for by assigning a probability x to a lattice site being occupied by a Mn ion—this enters the calculation when carrying out the sums over lattice sites and finally leads to the x dependence in Eq. (10). We should remark that the expressions borrowed from Van Vleck are for the secular (or diagonal) part of the dipolar Hamiltonian only. However, because of the strong isotropic exchange in these materials, we need to take into account the nonsecular or off-diagonal terms too, and this is accomplished by multiplying the final result by a factor of "$\frac{10}{3}$" (Ref. 17).

For the case of the D-M interaction, we take H_A to have the following form:

$$H_A=H_{\text{D-M}}=-2\sum_{\substack{i,j\\ i<j}}\mathbf{D}_{ij}\cdot(\mathbf{S}_i\times\mathbf{S}_j)\ , \quad \text{(A8)}$$

where $\mathbf{D}_{ij}$ is antisymmetric in i and j. Here, the linewidth is calculated from first principles using Eqs. (A3)–(A5). We use the same approximations as in the dipolar case, and carry out the calculation for the full D-M Hamiltonian to obtain the final result in Eq. (12).

*Present address: Department of Physics, University of Notre Dame, Notre Dame, IN 46556.

[1] J. K. Furdyna and N. Samarth, J. Appl. Phys. **61**, 3526 (1987).
[2] M. A. Butler, S. J. Martin, and R. J. Baughman, Appl. Phys. Lett. **49**, 1053 (1986).
[3] R. E. Kremer and J. K. Furdyna, Phys. Rev. B **32**, 5591 (1985).
[4] R. E. Kremer and J. K. Furdyna, J. Magn. Magn. Mater. **40**, 185 (1983).
[5] H. A. Sayad and S. M. Bhagat, Phys. Rev. B **31**, 591 (1985).
[6] S. B. Oseroff, Phys. Rev. B **25**, 6584 (1982).
[7] R. E. Kremer and J. K. Furdyna, Phys. Rev. B **31**, 1 (1985).
[8] P. W. Anderson and P. R. Weiss, Rev. Mod. Phys. **25**, 269 (1953).
[9] R. Kubo and K. Tomita, J. Phys. Soc. Jpn. **9**, 888 (1954).
[10] H. Mori and K. Kawasaki, Prog. Theor. Phys. (Kyoto) **28**, 971 (1962).

[11]E. Dormann and V. Jaccarino, Phys. Lett. **48A**, 81 (1974).
[12]P. M. Levy and R. Raghavan, J. Magn. Magn. Mater. **54-57**, 181 (1986).
[13]N. Samarth, Ph.D. thesis, Purdue University, 1986.
[14]D. R. Yoder-Short, U. Debska, and J. K. Furdyna, J. Appl. Phys. **58**, 4056 (1985).
[15]A. Abragam, *Principles of Nuclear Magnetism* (Oxford University Press, New York, 1983).
[16]D. L. Huber, Phys. Rev. B **31**, 4420 (1985).
[17]J. H. Van Vleck, Phys. Rev. **74**, 1168 (1948).
[18]J. Spalek, A. Lewicki, Z. Tarnawaski, J. K. Furdyna, R. R. Galazka, and Z. Obuszko, Phys. Rev. B **33**, 3407 (1986).
[19]B. E. Larson, K. C. Hass, and R. L. Aggarwal, Phys. Rev. B **33**, 1789 (1986).
[20]Y. Shapira and N. F. Oliveira, Jr., Phys. Rev. B **35**, 6888 (1987).
[21]B. E. Larson, K. C. Hass, H. Ehrenreich, and A. E. Carlsson, Solid State Commun. **56**, 347 (1985).
[22]T. Moriya, Phys. Rev. **120**, 91 (1960).
[23]We are deeply indebted to C. Henley for this suggestion.
[24]F. Keffer, Phys. Rev. **126**, 896 (1962).
[25]D. J. Chadi, Phys. Rev. B **16**, 790 (1977).
[26]W. Wu, G. Mozurkewich, and R. Orbach, Phys. Rev. B **31**, 4557 (1985).
[27]M. K. Hou, M. B. Salamon, and T. A. L. Ziman, Phys. Rev. B **30**, 5239 (1984).
[28]R. Kubo and T. Toyabe, in *Magnetic Resonance and Relaxation*, edited by R. Blinc (North-Holland, Amsterdam, 1967), p. 810.
[29]We would like to thank Professor M. B. Salmon for supplying the subroutines used in evaluating the Kubo-Toyabe line shapes.
[30]E. J. Ansaldo, D. R. Noakes, R. Keitel, S. R. Kreitzman, J. H. Brewer, and J. K. Furdyna, Phys. Lett. A **120**, 483 (1987).
[31]R. R. Galazka, S. Nagata, and P. H. Keesom, Phys. Rev. B **22**, 3344 (1980).
[32]J. Spalek, A. Lewicki, and Z. Tarnawski (unpublished).
[33]C. D. Amarasekara, R. R. Galazka, Y. Q. Yang, and P. H. Keesom, Phys. Rev. B **27**, 2868 (1983).
[34]Y. Q. Yang, P. H. Keesom, J. K. Furdyna, and W. Giriat, J. Solid State Chem. **49**, 20 (1983).
[35]B. Larson, Ph.D. thesis, Harvard University, 1988 (unpublished).